International Journal of
Structural Engineering and Analysis

ISSN: 2456-5326
Volume 10, Issue 1, 2024
DOI (Journal): 10.37628/IJSEA

https://journalspub.com/journal/ijsea/

Research IJSEA

Experimental and Numerical Analysis of RCC Beams Undergoing Four-Point Bending Tests: A Parametric Study of Acoustic Emission (AE) Techniques

Shubham Hatte[1,*], S.A. Bhalchandra[2]

Abstract

Reinforced concrete is a composite material where tensile reinforcement is added to increase its tensile strength since plain concrete is weak in tension. Reinforced concrete has far more complicated behavior than plain concrete. This is due to the microstructural changes in concrete as well as the interaction and link between concrete and steel. Micro-cracking of concrete and steel yielding are the two most common failure mechanisms in reinforced concrete. Reinforced cement concrete is a durable construction material, so it is used for decades. Concrete is a composite material; each of these material has different properties from each other. So knowledge of the properties of concrete, mainly at the loading stage, is necessary. To remain concrete in good condition, concrete should satisfy the limited state of serviceability and collapse. Assessing existing structures using non-destructive techniques is a significant research area in modern engineering due to its ability to estimate structural health without causing unwanted damage. Among the various established methods, acoustic emission (AE) analysis is gaining increasing interest in the scientific community. AE can detect the initiation of cracking processes, identify the types of cracks, and extract additional information from the specimens.

Keywords: AE – acoustic emission, SHM – structural health monitoring, UR – under reinforced, OR – over reinforced

INTRODUCTION

The acoustic emission (AE) approach is extensively used for structural health monitoring (SHM). One of its main advantages is that it can be applied without disrupting any processes associated with reinforced concrete (RC) structures. AE is a commonly used non-destructive material evaluation technique characterized by the generation of elastic waves due to the rapid release of energy from specific sources within a material. An AE approach can provide useful information about what's going on inside a material and is suited for online monitoring during the maintenance of structures and facilities. The AE sensor network captures the wave motion that occurs as a result of such damage events.

An AE technique is used without interrupting any processes that are associated with RCC structures. In the AE phenomenon, elastic waves are generated by the sudden release of energy from localized sources that are in the material. An AE technique can give some valuable information on what is happening inside the material, so this technique is suitable for online monitoring during the service of structures.

*Author for Correspondence
Shubham Hatte
E-mail: shubhamhatte1997@gmail.com

[1]Student, Department of Applied Mechanics, Government College of Engineering Chhatrapati Sambhajinagar, Maharashtra, India
[2]Professor, Department of Applied Mechanics, Government College of Engineering Chhatrapati Sambhajinagar, Maharashtra, India

Received Date: May 25, 2024
Accepted Date: June 11, 2024
Published Date: June 12, 2024

Citation: Shubham Hatte, S.A. Bhalchandra. Experimental and Numerical Analysis of RCC Beams Undergoing Four-point Bending Tests: A Parametric Study of Acoustic Emission (AE) Techniques. International Journal of Structural Engineering and Analysis. 2024; 10(1): 22–37p.

Modeling reinforced concrete using finite element software is intricate work since both the elastic and plastic properties of concrete in tension and compression are to be considered while creating an appropriate model. The simulation of the compressive behavior of concrete includes strain-softening, while the simulation of the tensile behavior of reinforced concrete includes tension softening, tension stiffening, and local bond effects. For plotting stress-strain curves of concrete in tension and compression, many numerical methods are available, but in this study, a finite element program, ABAQUS, is used to model the flexural behavior of the RCC beam since ABAQUS has the superior capability to represent the mechanical properties of concrete, including compressive and tensile strength in strain hardening and softening behavior and the characteristics related to steel reinforcement rebar.

For experimental validation, a four-point bending test was performed on the RCC beam. For the bending test on the beam. The stress concentration in the three-point bending test is small and concentrated under the center of the loading point, but the stress concentration in the four-point bending test is over a larger region. So it avoids premature failure. Therefore, in this study, a four-point bending test is preferred.

REVIEW OF ACOUSTIC EMISSION TECHNIQUE

Figure 1 shows the apparatus for the AE approach, which includes three stages of acquisition: detection, signal conditioning, and output. Below is a brief summary of the three steps.

The elastic waves traveling through the material are captured and converted to an electrical signal using low-output piezoelectric resonant sensors in the detection step. Pre-amplification, filtering, and signal processing are all part of the signal condition step. Pre-amplifiers increase the signals once they have been identified. The level of amplification is determined by the strength of the source, the application, and other factors. To remove noise from the sensor's operational range, frequency filters are used. Signal processing is used for digitalization and signal feature extraction, and the signals are translated from one format to another (Figure 2).

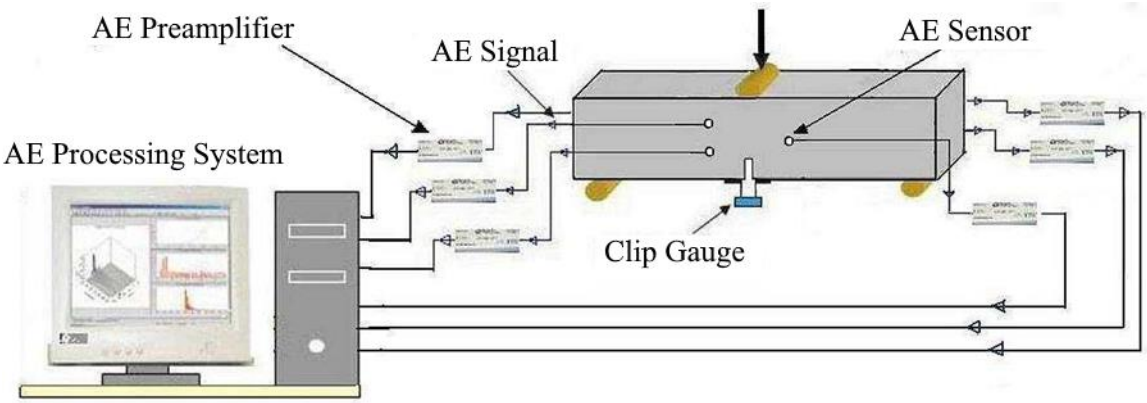

Figure 1. The apparatus for the AE approach.

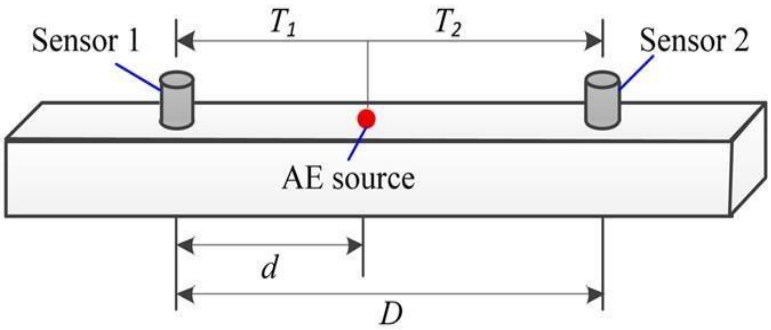

Figure 2. To remove noise from the sensor's operational range.

RA VALUES AND AVERAGE FREQUENCY

The RA value and average frequency are used to estimate the properties of AE signals. The AE parameters, such as rising time, maximum amplitude, counts, and duration, are used to determine the RA value and average frequency. The correlation between the RA value and the average frequency is used to classify crack types. An AE signal with a high average frequency and a low RA value is a tensile-type crack. A low average frequency and a high RA value characterize a shear-type crack. This criterion is used to categorize AE data that has been detected during the test on the concrete specimen (Figure 3).

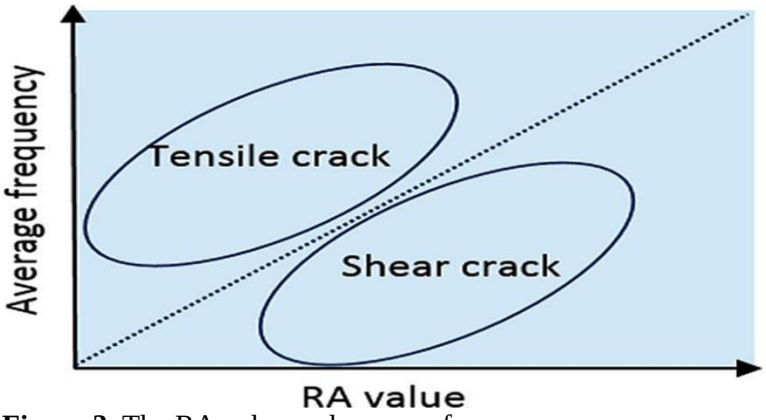

Figure 3. The RA value and average frequency.

FLEXURAL TEST ON REINFORCED CONCRETE BEAM

To determine the tensile strength of concrete indirectly, a flexural test is used. It tests the ability of a concrete beam or slab to resist loads against bending. The results of the flexural test on a concrete beam are expressed as a modulus of rupture value in Mpa. Flexural testing can be performed either as a four-point bending test (IS: 516 -1959) or a three-point bending test (Figures 4 and 5).

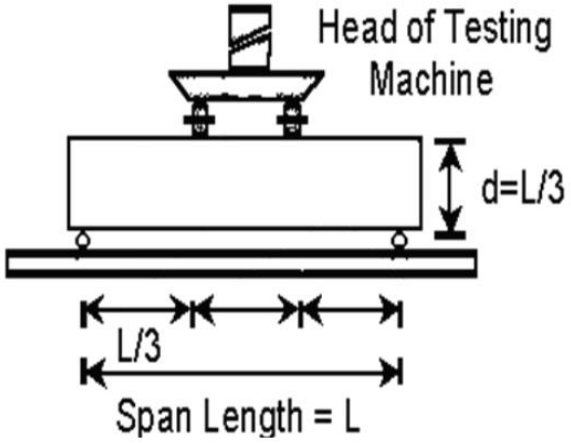

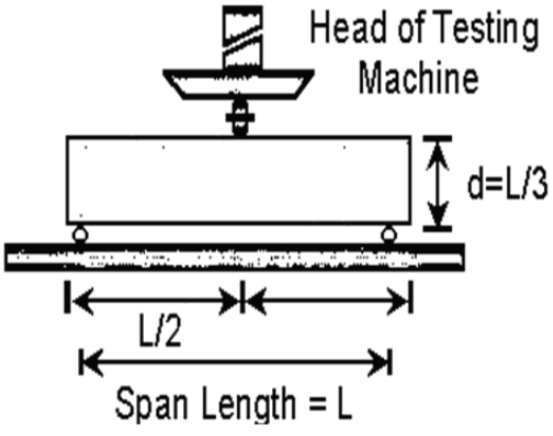

Figure 4. Test setup for the four-point bending test. **Figure 5.** Test setup for the three-point bending test.

According to IS: 516 -1959 the size of the specimen is square section with the size of 150 mm and the length should be greater than three times of the depth of the specimen. Indian standard code IS: 516 -1959 determined the size of the concrete specimen as square section of the size 150 mm, with length of 700 mm.

SAMPLE PREPARATION

Specimen Details

The experimental program consists of a total twelve RCC beams. The rectangular cross section of each beam is 150 mm x 150 mm, and the total length of each beam is 700 mm. Details of each beam

are illustrated in Tables 1 and 2. Out of twelve beams, six are cast with M25-grade concrete, and out of those six beams, three are designed as under-reinforced while the remaining three are designed as over-reinforced beams. Similarly, the remaining six beams are cast with M30-grade concrete (Tables 1 and 2).

Table 1. Description of specimen.

Beam	Cross-Section	Grade of Concrete	Bottom Steel	Top Steel	Grade of Longitudinal Steel	Type of Section
UR1-25	150 mm X 150 mm	M25	2-12 mm dia. bars	2-10 mm dia. bars	Fe 500	Under-reinforced
UR2-25			2-12 mm dia. bars			
UR3-25			2-12 mm dia. bars			
OR1-25			3-12 mm dia. bars	2-10 mm dia. bars		Over-reinforced
OR2-25			3-12 mm dia. bars			
OR3-25			3-12 mm dia. bars			
UR1-30	150 mm X 150 mm	M30	2-12 mm dia. bars	2-10 mm dia. bars	Fe 500	Under-reinforced
UR2-30			2-12 mm dia. bars			
UR3-30			2-12 mm dia. bars			
OR1-30			3-12 mm dia. bars	2-10 mm dia. bars		Over-reinforced
OR2-30			3-12 mm dia. bars			
OR3-30			3-12 mm dia. bars			

Table 2. Components of mix (kg/m3).

Material	M25	M30
Cement	448	450
M-sand	627	585.34
20 mm aggregate	680.2	668.8
10 mm aggregate	451.8	444.25
Water	217.9	190.61

Objectives

The objectives of this study are to:

1. Analyze the structural response (AE signals) due to different acoustic emission sources.
2. Perform experimental investigations on the reinforced concrete beam using a four-point bending test.
3. Model the reinforced concrete beam for a four-point flexural test using the finite element tool (ABAQUS) and compare the results obtained from numerical and experimental investigations.

LITERATURE REVIEW

Acoustic emission is one of the most effective techniques used in non-destructive evaluation of materials because it has the ability to detect, localize, and then monitor active crack growth. There is a lot of need for research in the qualitative and quantitative assessment of damage (nature, location, and

severity) based on the acquired data on acoustic emission. The acoustic emission technique can be used for the analysis of reinforced concrete beams under a four-point bending test [1–13]. A finite element model for the same can be prepared, which will give reliable results. In brief, summarizing the work done by different scholars and researchers.

Murthy et al. [1] performed an experiment on AE monitoring of an RCC beam subjected to four-point bending. Here, the damage mechanism of RC beams with different percentages of steel is studied. Four zones of damage, such as the formation of micro-cracks, visible cracks, steel yielding, and concrete crushing, are classified. It was found that as the level of damage increased, AE parameters like count hits, rise time, AE energy, and duration increased, which coincided with visual observation.

Kyriazopoulos et al. [2] performed an analysis of acoustic emissions from cement beams when applying three-point bending with different loading rates. The experiment is carried out at 6 different loading rates, varying from 22 N/s to 87 N/s. For each case, while approaching the near-failure stage, load variation shows similar variation. Loads higher than 50 N/s show dynamic behavior. The beam specimen is tested 90 days after the casting. As the loading rate increases, number of events decreases.

Stavrakas et al. [3], performed three-point bending tests. The mortar is made of white cement. After 90 days of preparation, the specimen was tested. Six repetitions of increasing load levels were carried out until the specimen failed. The Kaiser effect can be apparent in the results of experiments. The cumulative AE energy is displayed against the normalized load. When the applied load approaches the maximum load of the preceding loading loop, the AE energy increases significantly. Because this is a preliminary method, the outcomes are predominantly qualitative at this point. To derive quantitative and statistically analyzed conclusions, more experimental evidence is required.

Roja et al. [7] used ABAQUS to conduct analytical research on the flexural behavior of concrete beams reinforced with steel rebars. When a reinforced concrete beam is subjected to flexural loading, this research compares numerical and experimental results. The RCC beam, which had been tested in an earlier study by the author, was simulated using the ABAQUS program for validation. The results of this study reveal that the experimental results and the deflection, compressive strain of concrete, and tensile strain of reinforcement from the finite element method (FEM) model are closely correlated. In this study, only one beam is studied for various parameters like load vs. deflection curve, compressive and tensile strain of reinforcement, etc.

Mohammad et al. [8] analyzed the data using the finite element approach and compared it to the experimental data. Six beams are cast for the experimental portion. The load that generated the initial fracture, ultimate carrying capacity, load and deflection behavior at the midspan of beams, crack pattern, and beam damage behavior were all considered in this study. Finally, the author discovered that the experimental and simulation results were in good agreement, demonstrating the efficiency of the finite element method for simulating beam flexural performance.

Chowdary et al. [9] investigated the flexural behavior of reinforced concrete beams by experimental analysis and inquiry. In this study, two plane concrete beams and six reinforced concrete beams are cast and tested. Two of the six reinforced concrete beams are under-reinforced, two are over-reinforced, and two are balanced. Deflection, stress in steel, the load at which the first crack occurs, and the ultimate load are all variables to consider. The results were then compared to those obtained using a finite element model. The ultimate load-carrying capacity of a plane concrete beam is 0.14 times that of an under-reinforced beam, according to the author. Also, reinforcement in the under-reinforced part reaches its ultimate stress, whereas reinforcement in the over-reinforced segment reaches 87 percent of its ultimate stress.

Rao et al. [10] performed a comparative study on the analysis of plain and RC beam using ABAQUS. In this study, both plain and reinforced concrete beams were cast and tested with the same dimensions

and grade in both cases. A three-point bending test is carried out, and the results, like the stress strain curve, are plotted and compared with the result of finite element model. Then it was observed that plain concrete, being weak in tension, fails at lower loads and can sustain lower deflection as compared to RCC beams. In the case of both RCC and plain concrete beams, failure starts at the center of the beam.

Rahman et al. [11] analyzed and validated a reinforced foam concrete beam containing partial by cement replacement. In this study, a three-dimensional non-linear simulation of the RCC beam was done using the FEM program ABAQUS. A four-point bending test is used for the flexural test of the beam. Here, RCC foamed concrete beams consisting of palm oil fuel and eggshell powder with a certain percentage as a partial replacement for the cement. Here, a parametric study with variation in the length is done where steady increment results in terms of load capacity have been observed. For numerical analysis, the concrete damage plasticity model (CDP) was showing good agreement to determine the failure behavior of foamed concrete. Further parametric studies can be done as a future scope for this study.

Zhang et al. [12] performed a numerical investigation of RC beams strengthened with UHPFRC (ultra high-performance fiber reinforced concrete). In this study, a four-point bending test is simulated using the FEM software ABAQUS, and the results from this numerical analysis were compared with experimental data from some previous studies. In most of the literature, it is found that a 2-noded linear 3D truss element is used to simulate rebar in a finite element model. But in this study, an alternate 3D finite element model was developed using ABAQUS, in which the bond between concrete and rebar was modeled using the cohesive surface interaction method, which was found to be a better approach for simulation. Here the load displacement curve for both experimental and numerical analysis is plotted, and both are nearly matching. An alternative technique of cohesive surface bonding gives good accuracy.

Mohamad MZ et al. [13] performed the non-linear analysis of reinforced concrete beam bending failure experimentation based on ABAQUS. In this study, non-linear analysis of reinforced concrete beams was conducted using the finite element program ABAQUS. Here, a simply supported concrete beam is used for the analysis. A plasticity model for concrete damage is used in the analysis. Finally, results from experimentation and numerical analysis are compared, and then, in conclusion, the reason for the difference between experimental and numerical results are discussed. It has been concluded that finite element simulation of reinforced concrete has a high degree of similarity with the actual results of experiments.

RESULT AND DISCUSSION

The load displacement curve for different cases is shown in Figures 6–9.

Results for Under-Reinforced Beam of Grade M25

After performing a four-point bending test on the UR beam of grade M25 and measuring the mid-span deflection of the beam, the load vs. mid-span deflection curve is plotted as shown in Figure 6. The test performed is displacement-controlled, in which the rate of loading is 0.01 mm/min. After calculating the maximum load-carrying capacity and corresponding deflection, it was decided to load the beam up to a span deflection of 15 mm [11–16].

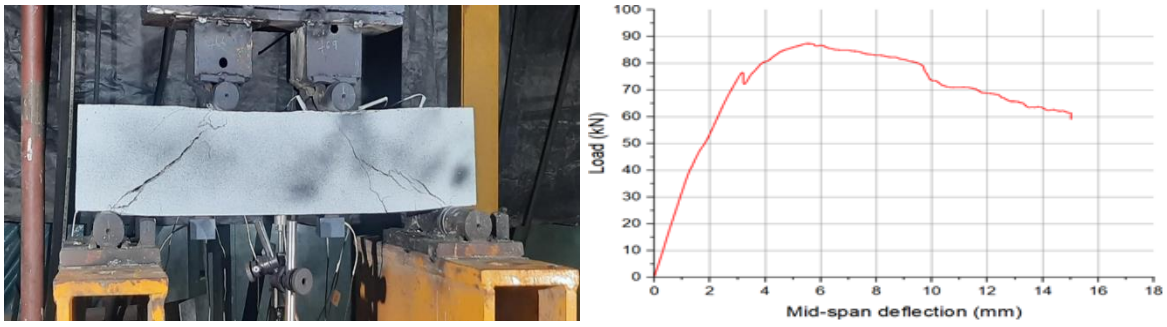

Figure 6. Results for the under-reinforced beam of grade M25.

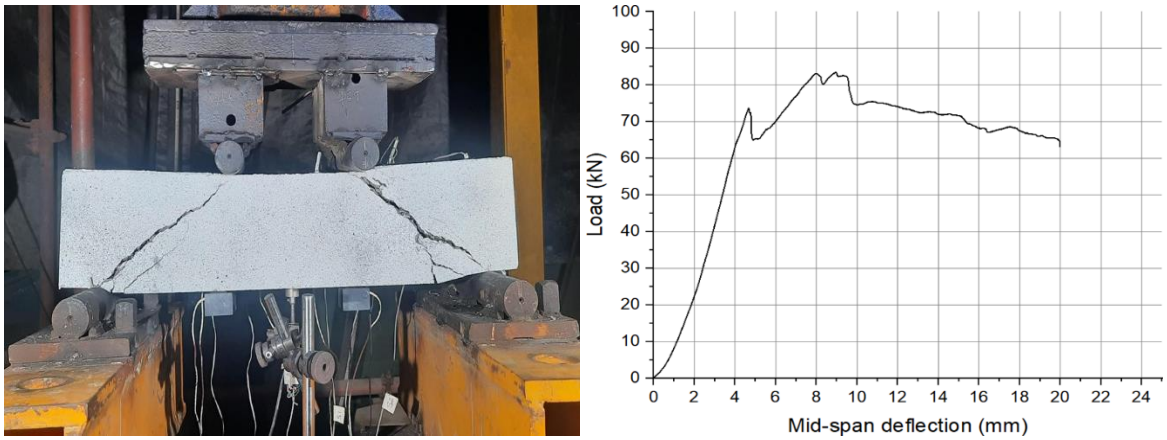

Figure 7. Results for or beam of grade M25.

The first tensile crack is obtained at a load of 17.8 kN. Since only nominal shear reinforcement is provided in the beam, as expected, after loading, the beam starts getting shear cracks, as shown in the picture above. Then the maximum load-carrying capacity of the beam is found to be 87.43 kN, and the corresponding mid-span deflection when the load reaches the capacity of 87.43 kN is 5.59 mm.

Results for or Beam of Grade M25

The load-displacement curve consists of three stages: the elastic stage, the second stage, which includes a sudden jump and drop of load bearing due to crack initiation, and the third stage, which includes post-crack residual or simply hardening state. In the first stage, both concrete and reinforcement take on loads, so the curve is in the elastic stage. Then due to damage to concrete occurs, so load bearing suddenly decreases, and then momentary redistribution occurs. Then the slope of the curve changes, and load bearing increases in the hardening state. Then, after reaching the maximum load-carrying capacity of the beam, its load-bearing decreases, as shown in the above graph.

Results for Under-Reinforced Beam of Grade M30

After performing a four-point bending test on the UR beam of grade M30 and measuring the mid-span deflection of the beam, the load vs. mid-span deflection curve is plotted as shown in Figure 7. The test performed is displacement-controlled, in which the rate of loading is 0.01 mm/min. After calculating the maximum load-carrying capacity and corresponding deflection, it was decided to load the beam up to a mid-span deflection of 20 mm.

The first tensile crack is obtained at a load of 18 kN. Since only nominal shear reinforcement is provided in the beam, as expected, after loading, the beam starts getting shear cracks, as shown in the picture above. Then the maximum load-carrying capacity of the beam is found to be 104.94 kN, and the corresponding mid-span deflection when the load reaches the capacity of 104.94 kN is 9.88 mm.

Results for Over-Reinforced Beam of Grade M30

After performing a four-point bending test on the OR beam of grade M30 and measuring the mid-span deflection of the beam, the load vs. mid-span deflection curve is plotted as shown in Figure 8. The test performed is displacement-controlled, in which the rate of loading is 0.01 mm/min. After calculating the maximum load-carrying capacity and corresponding deflection, it was decided to load the beam up to a mid-span deflection of 20 mm. The first tensile crack is obtained at a load of 15 kN. Since only nominal shear reinforcement is provided in the beam, as expected, after loading, the beam starts getting shear cracks, as shown in the picture above. Then the maximum load-carrying capacity of the beam is found to be 98.46 kN, and the corresponding mid-span deflection when the load reaches the capacity of 98.46 kN is 9.19 mm.

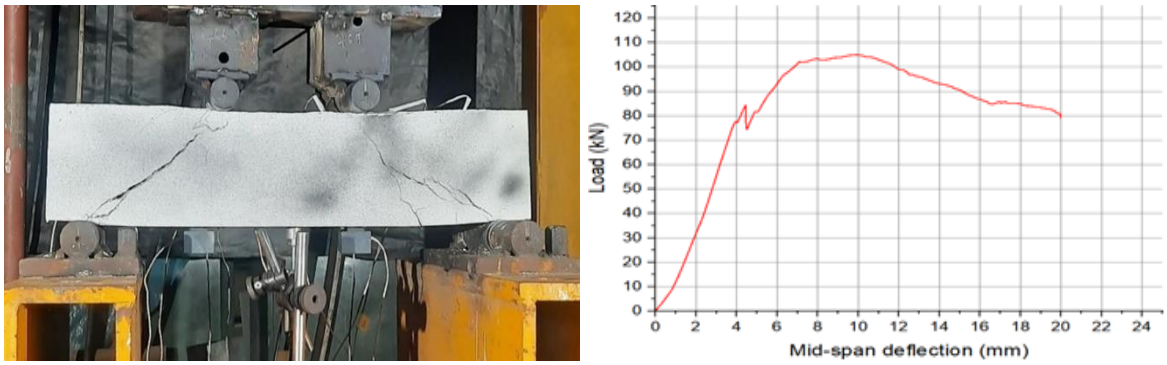

Figure 8. Results for under-reinforced beam of grade M30.

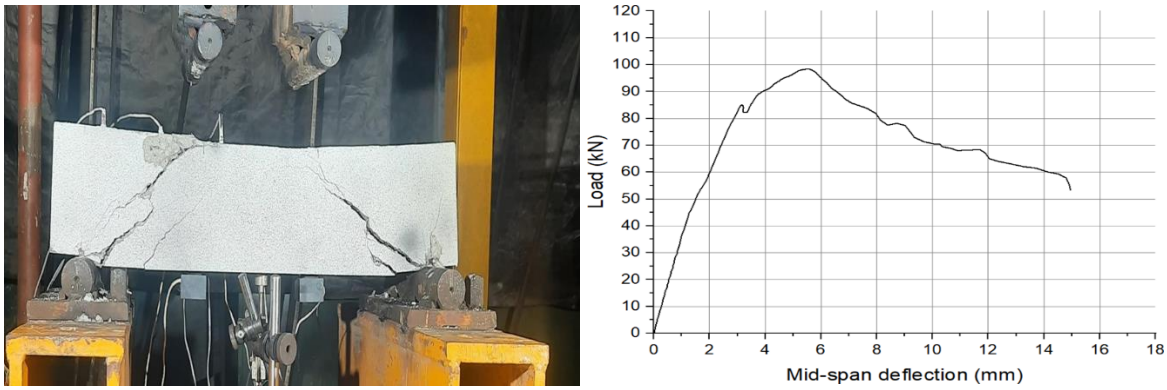

Figure 9. Results for over-reinforced beam of grade M30.

The load-displacement curve consists of three stages: the elastic stage, the second stage, which includes a sudden jump and drop of load bearing due to crack initiation, and the and the third stage, which includes post-crack residual or simply hardening state. In the first stage, both concrete and reinforcement take on loads, so the curve is in the elastic stage. Then due damage to concrete occurs, so load bearing suddenly decreases, and then momentary redistribution occurs. Then the slope of the curve changes, and load bearing increases in the hardening state. Then, after reaching the maximum load-carrying capacity of the beam, its load-bearing decreases, as shown in the above graph in Table 3.

Table 3. Comparison of results of under-reinforced and over-reinforced beams (experimental).

Name of Beam	Maximum Load-Carrying Capacity (kN)	Corresponding Displacement (mm)
UR-25	87.43	5.59
OR-25	83.53	8.94
UR-30	104.94	9.88
OR-30	98.46	9.19

The load-carrying capacity of an under-reinforced beam is higher as compared to an over-reinforced beam. The displacement corresponding to that maximum load is greater for an over-reinforced beam as compared to an under-reinforced beam.

Acoustic Emission (AE) Parametric Analysis

Parametric analyses are shown in Figures 10–13.

Parametric Analysis for UR-25 Beam

In phase 1, all the plotted points are in the tension zone because of a tensile crack on the surface of the beam. In phase 2, some plotted points are seen on the shear zone, indicating the transformation of the tensile crack into a shear crack. Then, in phase 3, plotted points in the shear zone increased. For the

shear zone, there are fewer plotted points, which are not expected since, in visual observation, we have observed shear cracks.

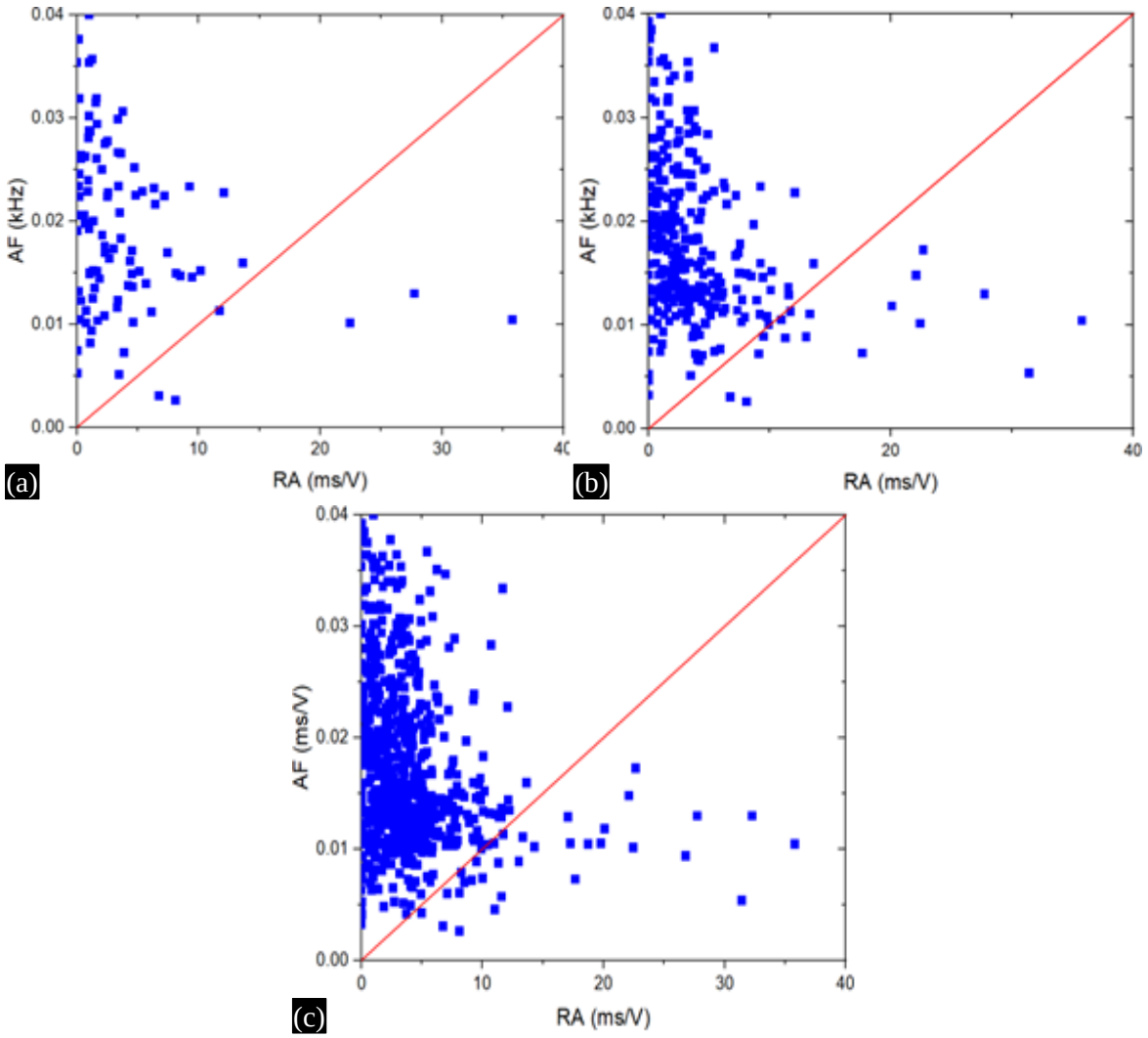

Figure 10. Parametric analyses for UR-25 beam (a) phase 1, (b) phase 2, (c) phase 3.

Parametric Analysis for OR-25 Beam

In phase 1, all the plotted points are in the tension zone because of a tensile crack on the surface of the beam. In phase 2, some plotted points are seen on the shear zone, indicating the transformation of the tensile crack into a shear crack. Then, in phase 3, plotted points in the shear zone increased. The concentration of hits at the tensile zone starts increasing during the formation of a shear crack, but at the shear zone, this increment is slightly less. This may happen due to the formation of tensile cracks that first initiate before they get converted into shear cracks.

Parametric Analysis for UR-30 Beam

In phase 1, all the plotted points are in the tension zone because of a tensile crack on the surface of the beam. In phase 2, some plotted points are seen on the shear zone, indicating the transformation of the tensile crack into a shear crack. Then, in phase 3, plotted points in the shear zone increased, observed shear crack, the concentration of hits at the tensile zone starts increasing during the formation of the shear crack, but at the shear zone, this increment was slightly less. This may happen due to the formation of tensile cracks that first initiate before they get converted into shear cracks.

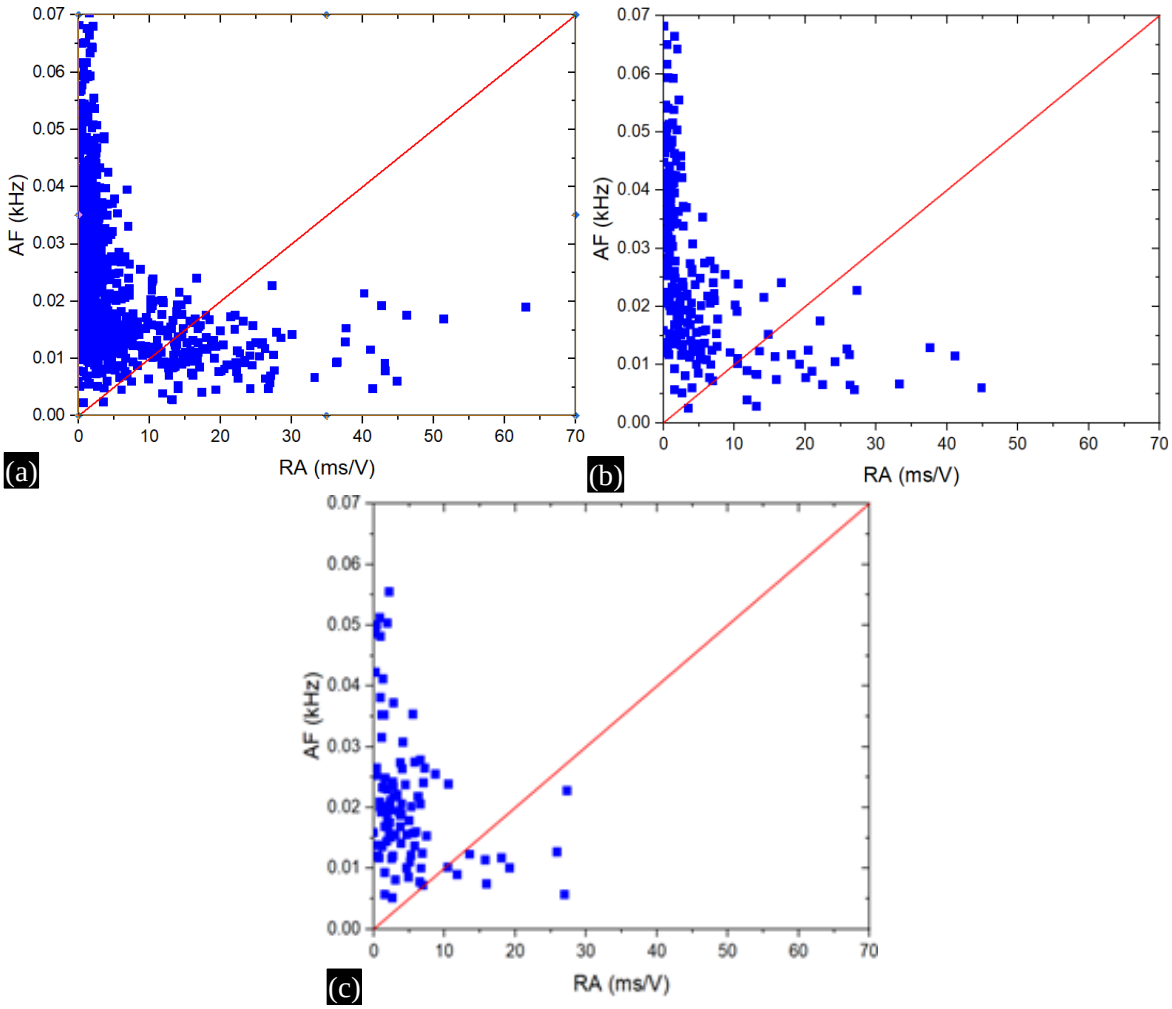

Figure 11. Parametric analyses for OR-25 beam (a) phase 1, (b) phase 2, (c) phase 3.

Parametric Analysis for OR-30 Beam

In phase 1, all the plotted points are in the tension zone because of a tensile crack on the surface of the beam. In phase 2, some plotted points are seen on the shear zone, indicating the transformation of the tensile crack into a shear crack. Then, in phase 3, plotted points in the shear zone increased. For the shear zone, there are fewer plotted points, which is not expected since, in visual observation, we have observed shear cracks. The concentration of hits at the tensile zone starts increasing during the formation of a shear crack, but at the shear zone, this increment is slightly less. This may happen due to the formation of tensile cracks that first initiate before they get converted into shear cracks.

Above Figure 14 shows the number of hits for different beams and for different phases in the experiment. From this graph, we can see that the number of hits is highest for each type of beam in phase 2 as compared to phases 1 and 3. This may be due to a formation crack in phase 2. Over-reinforced beams show a higher number of hits as compared to under-reinforced beams for both M25 and M30 grades of concrete. Beams with M30-grade concrete shows fewer hits as compared to M25-grade concrete. This may be due to less crack formation at the initial stage in the case of a beam with a higher strength of concrete as compared to a beam with a comparatively lower strength of concrete (Figure 14).

Simulation Results

Simulation results are shown in Figure 15 and Table 4.

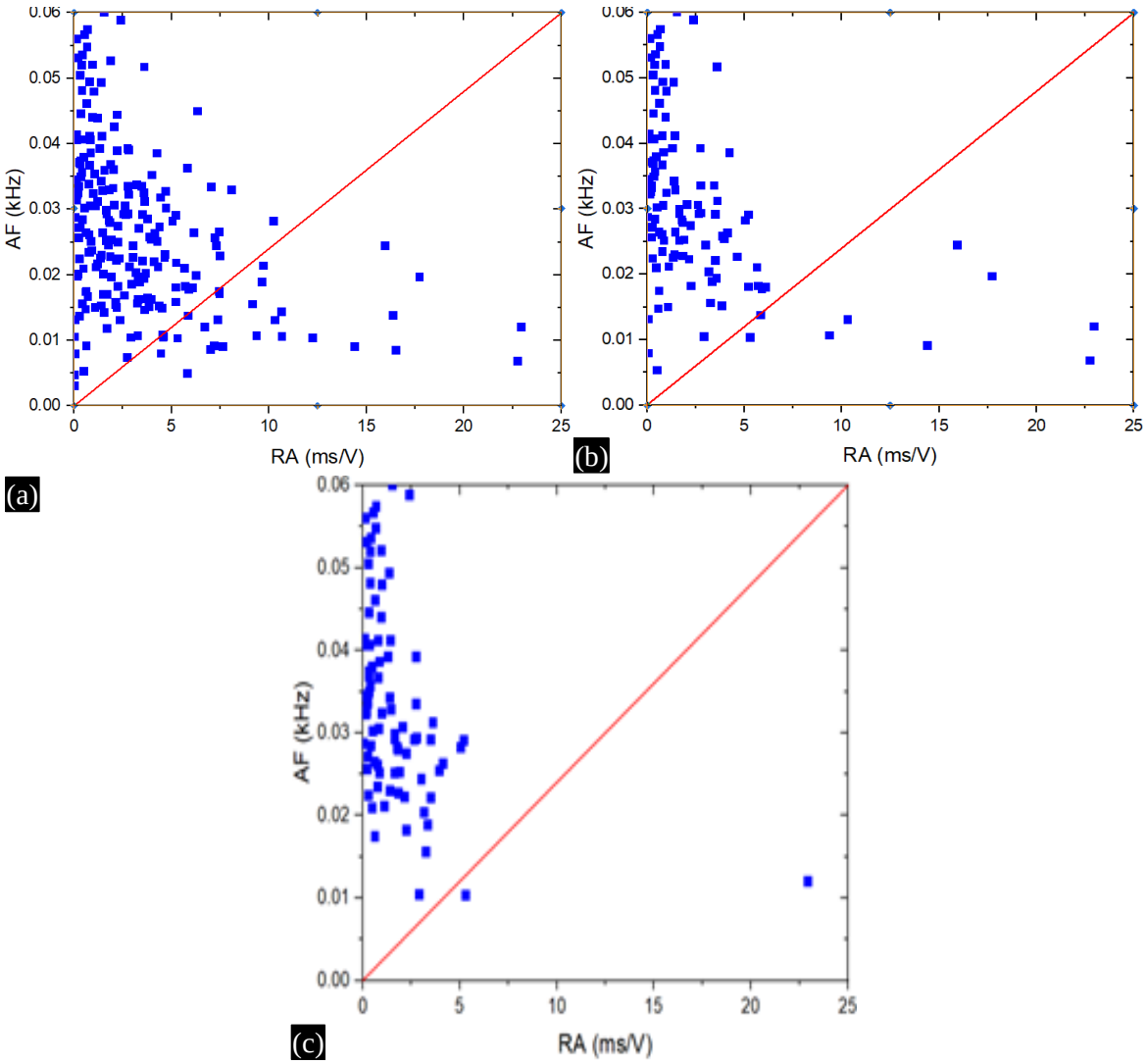

Figure 12. Parametric analyses for UR-30 beam (a) phase 1, (b) phase 2, (c) phase 3.

From the above Table 4, it states that the load-carrying capacity of an under-reinforced beam is higher as compared to an over-reinforced beam. The displacement corresponding to that maximum load is greater for an over-reinforced beam as compared to an under-reinforced beam.

Comparison for Experimental and Simulation Results

It shows a comparison of the experimental and simulation results of various beams. In all these graphs up to the elastic limit, both experimental and simulation results are perfectly matched. After that point, experimental results show quite good agreement with simulation results. All experimental graphs show a sudden decrease in the stiffness of the beam, but the same trend is not observed in the simulation results. This may be due to the assumption of homogenous material in ABAQUS modeling (Figures 16 and 17).

Table 4. Comparison of results of under-reinforced and over-reinforced beam (simulation).

Name of Beam	Maximum Load-Carrying Capacity (kN)	Corresponding Displacement (mm)
UR-25	85.38	4.94
OR-25	83.61	8.96
UR-30	104.67	6.90
OR-30	87.41	7.5

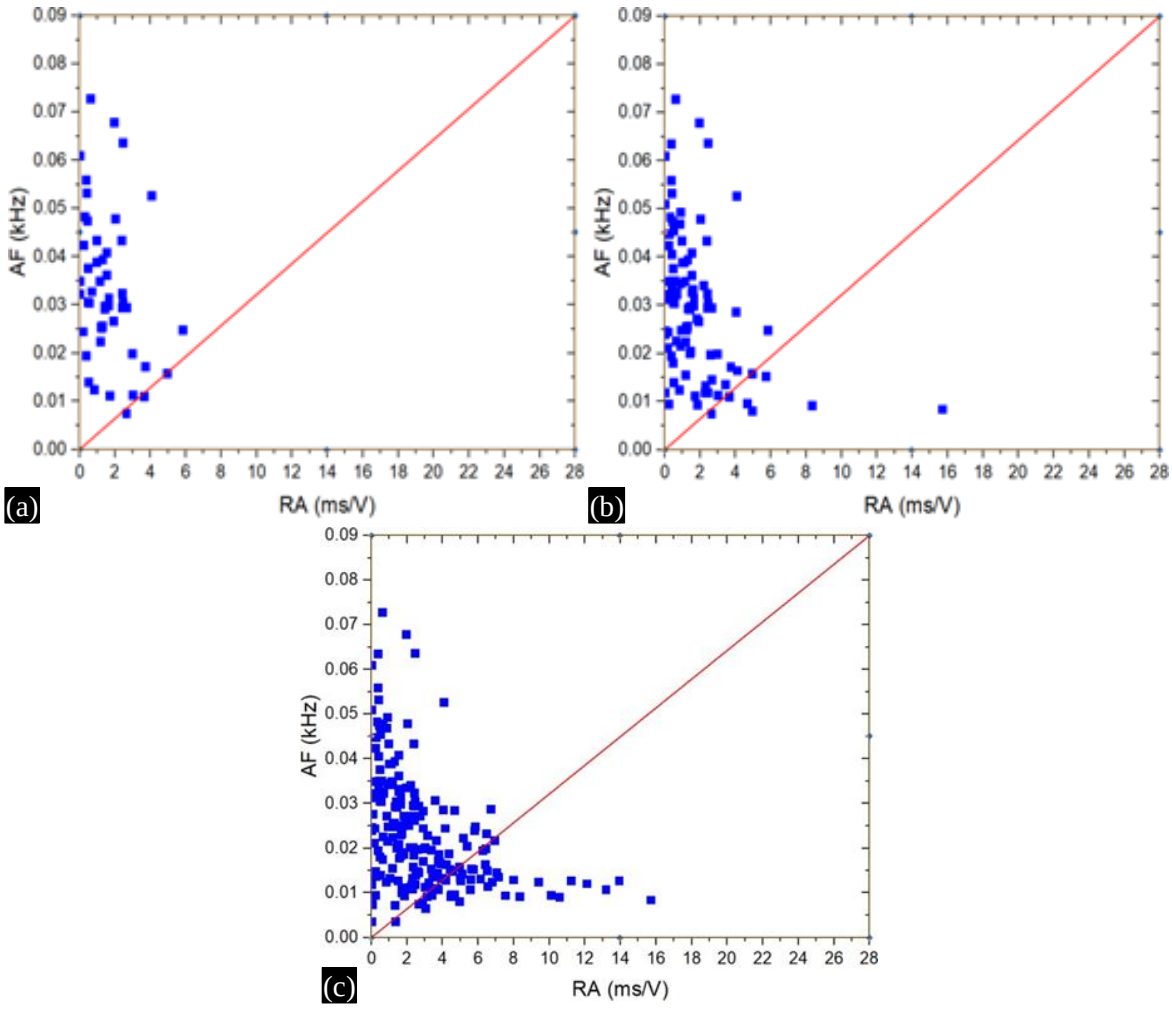

Figure 13. Parametric analyses for OR-30 beam (a) phase 1, (b) phase 2, (c) phase 3.

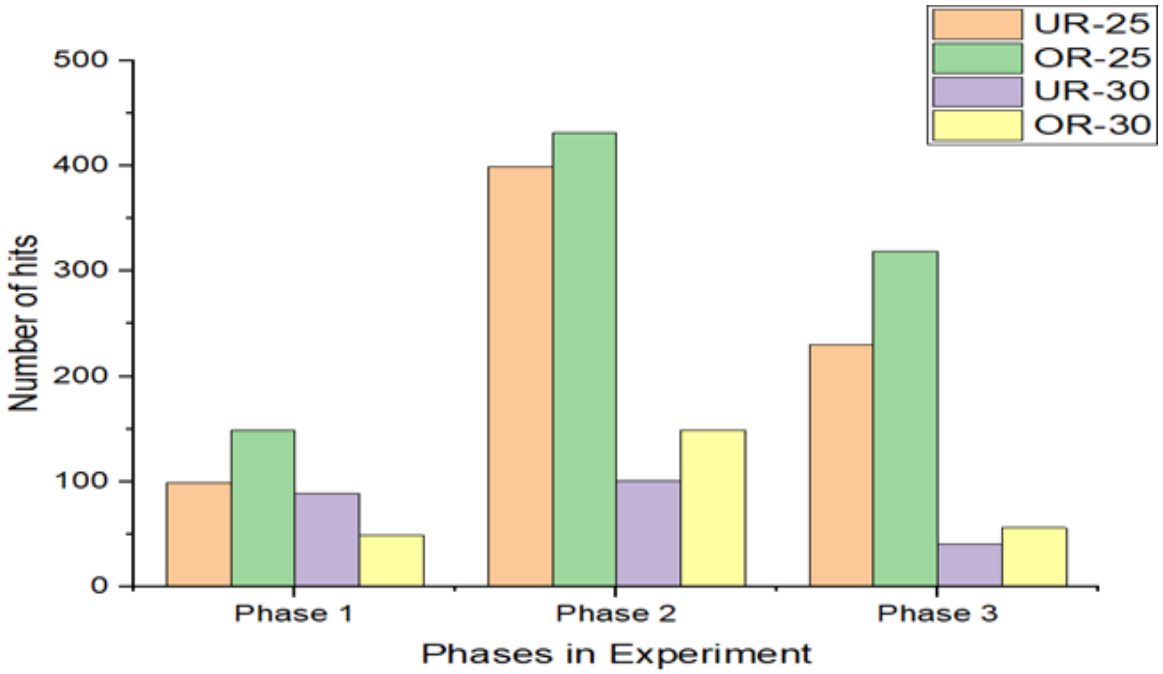

Figure 14. Different beams and for different phases in the experiment.

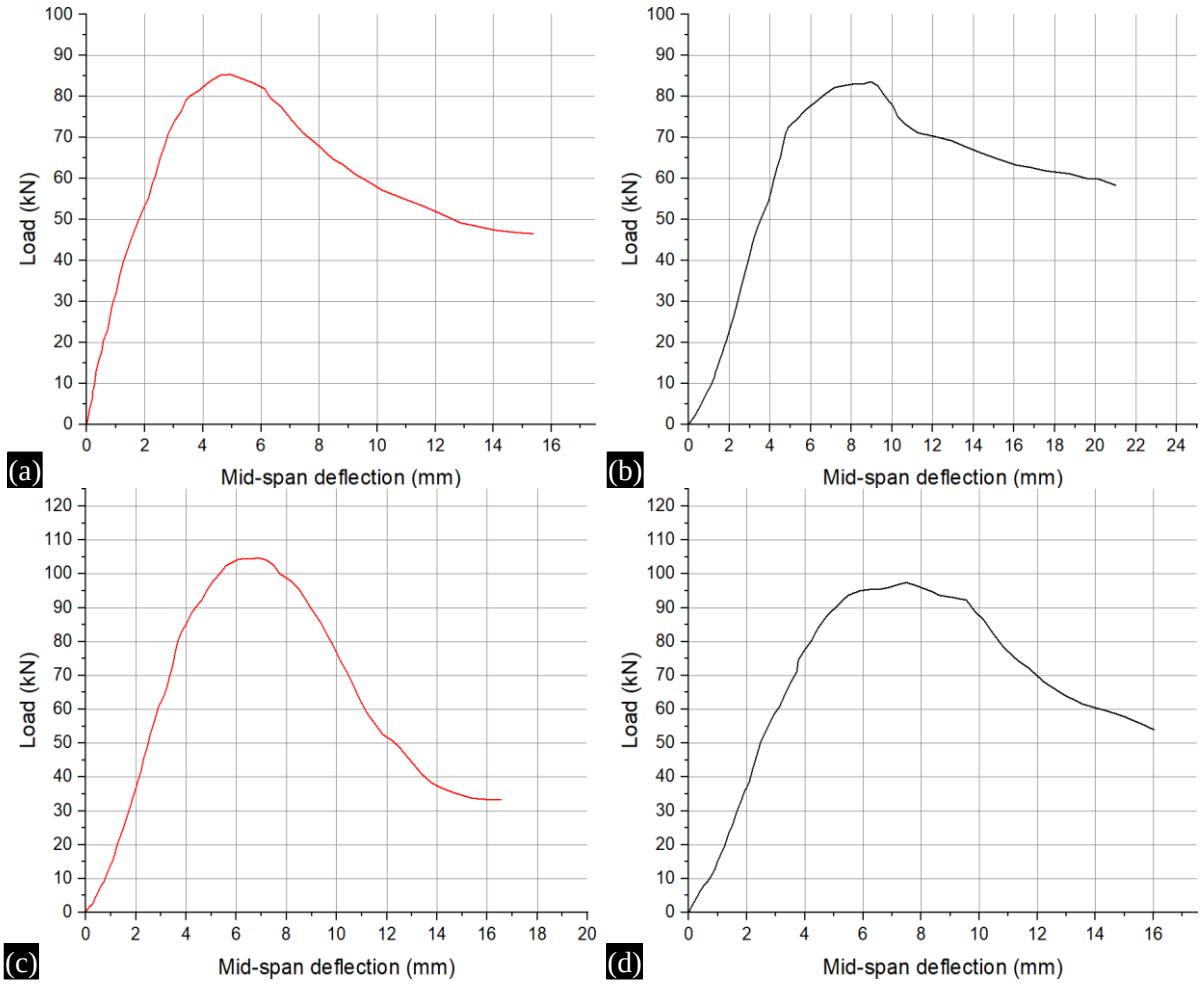

Figure 15. Simulation results. (a) results for UR-25 beam, (b) results for OR-25 beam, (c) results for UR-30 beam, (d) results for OR-30 beam.

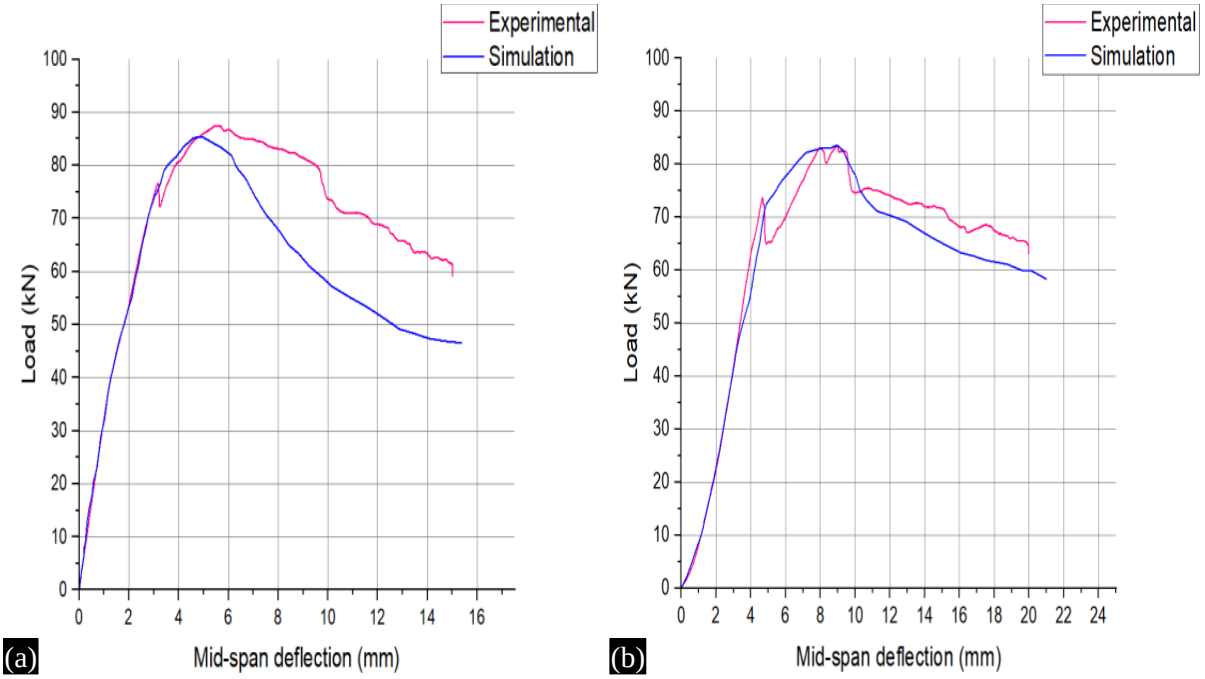

Figure 16. Comparison of results for (a) UR-25 beam, (b) OR-25 beam.

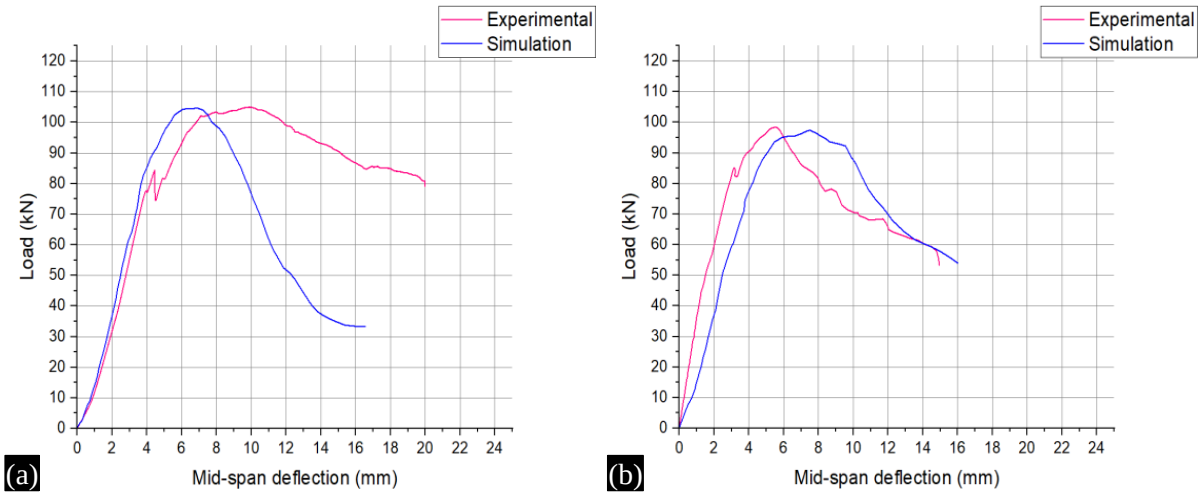

Figure 17. Comparison of results for (a) UR-30 beam, (b) OR-30 beam.

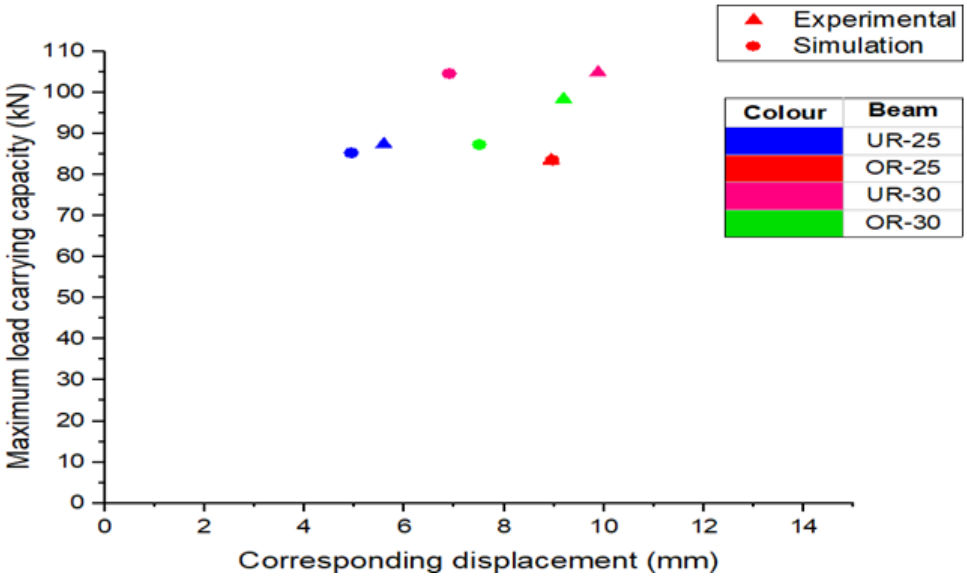

Figure 18. Maximum load-carrying capacity and corresponding displacement for different types of beams.

Summary

Above Figure 18 shows the relationship between maximum load-carrying capacity and corresponding displacement for different types of beams that are tested experimentally and simulated. From this, we can say that for the UR-25 and OR-25 beams, both experimental and simulation results show very good agreement, while for the UR-30 and OR-30, experimental and simulation results are a little different from each other. This shows that beams with M30 grade of concrete show more deviation in experimental and numerical results as compared to beams with M25 grade of concrete (Figure 18).

CONCLUSIONS

Both experimental and analytical results show that the load-carrying capacity of reinforced concrete beams subjected to four-point bending loading increases with an increase in the grade of the concrete, which is quite obvious. Also, for the same length of beam, the same cross section, and the same grade of concrete, the beam of an under-reinforced section has more load-carrying capacity as compared to the beam of an over-reinforced section. Actually, according to IS 456:2000, the moment-carrying capacity of an over-reinforced beam should be high, but the results obtained are just the opposite, which may be due to the failure of the beam in shear.

After performing a parametric analysis of acoustic emission (AE), it was found that:

- Initially, tensile cracks are generated since in the RA vs. average frequency graph in phase 1, all plotted points are found in the tension region. This tension crack then transforms into a shear crack, which is in accordance with the AE result since plotted points are found in the shear region in phases 2 and 3 of loading.
- The results of the RA vs. average frequency graph well matched with the crack pattern that appeared on the surface of the reinforced concrete beam. So, it can be concluded that acoustic emission can be effectively used for the identification of the type of crack.
- As the grade of concrete (strength) increases, the concentration of plotted points decreases, indicating fewer cracks in reinforced concrete beams with greater strength as compared to beams with comparatively less strength.
- Over-reinforced section beams show a higher number of hits as compared to under-reinforced section beams, which shows that as the amount of reinforcement increases, the number hits also increases. This may be due to many reasons, like bond failure between steel and concrete, the crushing of concrete, or the cracking of concrete.

After comparing experimental results with analytical results, it was found that both results were quite similar. This shows that the finite element tool ABAQUS can be effectively used for the simulation of reinforced concrete beams under a four-point bending test. So a study of the same finite element tool can be used instead of an experimental study, so an expensive and time-consuming experimental study can be avoided.

Due to the use of concrete damage plasticity (CDP) as a material property in Abaqus, tension damage to reinforced concrete beams is obtained, which matches the visual observations observed on the surface of the beam during the test.

REFERENCES

1. Prem PR, Murthy AR. Acoustic emission monitoring of reinforced concrete beams subjected to four-point-bending. Appl Acoust. 2017;117:28–38. doi:10.1016/j.apacoust.2016.08.006.
2. Kyriazopoulos A, Stavrakas I, Anastasiadis C, Triantis D. Analysis of acoustic emissions from cement beams when applying three-point bending with different loading rates. Recent Res Mech Transp Syst. 2015:57–63.
3. Stavrakas I, Triantis D, Kourkoulis SK, Pasiou ED, Dakanali I. Acoustic emission analysis of cement mortar specimens during three point bending tests. Lat Am J Solids Struct. 2016;13(12):2283–2297. doi:10.1590/1679-78252486.
4. Colombo IS, Main IG, Forde MC. Assessing damage of reinforced concrete beam using b-value analysis of acoustic emission signals. J Mater Civ Eng. 2003;15(3):280–286. doi:10.1061/(ASCE)0899-1561(2003)15:3(280).
5. Sagar RV. Acoustic emission characteristics of reinforced concrete beams with varying percentage of tension steel reinforcement under flexural loading. Case Stud Constr Mater. 2017;6:162–176. doi:10.1016/j.cscm.2017.01.002.
6. Yassin A. Acoustic emission non-destructive testing. 2020. doi:10.13140/RG.2.2.29388.85120/1.
7. Roja SY, Magudeaswaran P, Dharma MS, Eswaramoorthi DP. Analytical study on flexural behavior of concrete beams reinforced with steel rebars by ABAQUS. Int J Res Innov Eng Technol. 2016;57(3):1693–1712.
8. Mohammad GK, Sarasam KF, Korkes IN. Modeling the flexural performance of reinforced concrete built-up beams. IOP Conf Ser Mater Sci Eng. 2020;745(1):012108. doi:10.1088/1757-899X/745/1/012108.
9. Chowdary PHA, Bhuvanagiri S. Experimental analytical and investigation of flexural behavior of reinforced concrete beam. Int J Adv Sci Technol Eng Manag Sci. 2016;2(12):45–52.
10. Rao CK, Raju PP, Babu TNS. Comparative study on analysis of plain and RC beam using ABAQUS. Int J Civ Eng Technol. 2017;8(4):1531–1538.

11. Rahman AF, Goha WI, Mohamada N, Kamarudin MS, Jhatialb AA. Numerical analysis and experimental validation of reinforced foamed concrete beam containing partial cement replacement. Case Stud Constr Mater. 2019;11:e00297. doi:10.1016/j.cscm.2019.e00297.
12. Zhang Z, Abbas EMA, Wang Y. Numerical investigation of RC beam strengthened with UHPFRC (ultra high performance fiber reinforced concrete). Case Stud Constr Mater. 2021;15
13. Mohamad MZ, Noor NM, Ahmad WNAW. Average frequency – RA value for reinforced concrete beam strengthened with carbon fibre sheet. MATEC Web Conf. 2016;47:02010. doi:10.1051/matecconf/20164702010.
14. Mirgal P, Pal J, Banerjee S. Online acoustic emission source localization in concrete structures using iterative and evolutionary algorithms. Ultrason. 2020;108:106211. doi:10.1016/j.ultras. 2020.106211.
15. Bureau of Indian Standards. IS 456: Plain and reinforced concrete – code of practice. New Delhi: BIS; 2000.
16. Bureau of Indian Standards. IS 10262: Guidelines for concrete mix design proportioning. New Delhi: BIS; 2009.

